

Sonication-induced self-assembly of polymeric porphyrin–fullerene: Formation of nanorings

Sara Riaz,¹ Wang Feng,² Ather Farooq Khan,³ Mian Hasnain Nawaz^{2,3}

¹Department of Chemical Engineering, COMSATS Institute of Information Technology, Lahore, Pakistan

²Shanghai Key Laboratory of Functional Materials Chemistry, College of Materials Science and Engineering, East China University of Science and Technology, Shanghai, People's Republic of China

³Interdisciplinary Research Centre in Biomedical Materials, COMSATS Institute of Information Technology, Lahore, Pakistan

Correspondence to: M. H. Nawaz (E-mail: mhnawaz@ciitlahore.edu.pk)

ABSTRACT: In this article, we detail the sonication-induced self-assembly of polymeric porphyrin and fullerenes into distinct nanorings in solution form. The formation of these trenchant superstructures was the result of the delicate choice of different assembly protocols, solvents, and polymeric tails associated with porphyrin and fullerene. In this study, the sonication supposedly directed the lateral aggregation into uniform ring formation. The sonication time was found to be the key parameter in ring formation. Furthermore, the flexibility of polymeric arms and electronic interactions of porphyrin–fullerene gave rise to synergistically enhanced molecular interactions, and this resulted in discrete morphologies. Key optical data, including the absorption maxima of the complexes, and microscopic studies attested to the nature and morphology of the self-assembled complexes. This introduction of polymeric arms and sonication protocols in the porphyrin self-assembly was expected to allow the easy formation of diverse morphologies. Because of the facile fabrication process and uniform morphology, the resulting composite architectures might show promising applications in drug-delivery and advance materials. © 2016 Wiley Periodicals, Inc. *J. Appl. Polym. Sci.* **2016**, *133*, 43537.

KEYWORDS: graphene and fullerenes; morphology; nanotubes; self-assembly

Received 29 October 2015; accepted 12 February 2016

DOI: 10.1002/app.43537

INTRODUCTION

The bottom-up assembly of individual molecules by noncovalent interactions, which are typically reversible and weak, is sensitive to different variables, including the solvent polarity, temperature, pH, and concentration.¹ In this line of research, self-assembly has proved a fundamental strategy for building hierarchical structures with potential applications in smart materials and living systems.² It has been used as a powerful tool for the preparation of well-ordered and stable organic, inorganic, and polymeric nano- and micro-objects. It has provided the possibility for the development of numerous complex architectures ranging from one-dimensional to three-dimensional and starting from the individual chemical building blocks and sparked a very active field of current research.³ The properties of such self-assembled architectures depend strongly on their morphology; hence, the understanding of the dynamics, design, arrangement, and number of units is crucial for their applications.⁴ Morphological investigations could provide excellent model systems for different applications, especially in low-dimensional devices. However, the achievement of uniform complex dimensions remains a challenge. Similarly, the self-

assembly of porphyrin has attracted intense interest as a general route to the fabrication of nano-architectures for a wide range of applications. Amphiphilic porphyrins can be self-assembled into J-aggregates and nanotubes; such two-dimensional J-aggregates can be formed via distance- and orientation-dependent geometries of monomers.^{5,6} Hence, to get most of the functions and properties of porphyrin, the morphological studies are of paramount importance.⁷ Depending on the different parameters, including the concentration, solvent, temperature, and protocol of assembly, complex hierarchical morphologies are produced. Self-assembly enables the use of polymers as efficient and site-specific drug carriers because of their intrinsic properties of encapsulating a wide range of guest molecules; this can be controlled by various physical parameters.⁸ Because of its selective solubility profile in commonly used solvents and specific molecular interactions, porphyrin is challenging in the fabrication of controlled and well-ordered nanostructures. Numerous researchers have been inspired by the nature of such processing of porphyrin, and this has become a hot topic of recent research.⁹ Many structure-directing additives and parameters have been used in this context. Very recently, we

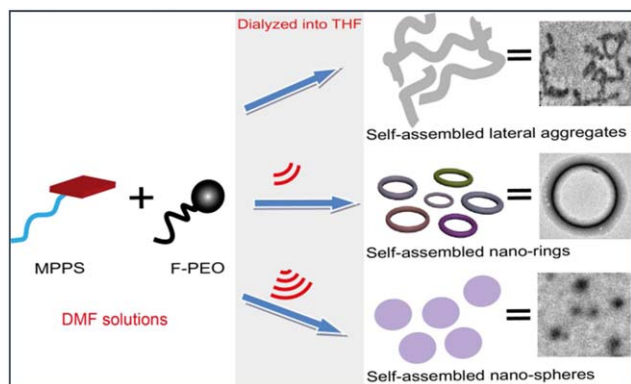


Figure 1. Schematic representation of the complex architectures of MPPS and F-PEO with various self-assembly protocols. [Color figure can be viewed in the online issue, which is available at wileyonlinelibrary.com.]

reported¹⁰ the formation of nanorings via the drop casting of a mixture of 5,10,15,20-tetrakisphenyl porphine zinc and 4,4'-bipyridine on copper grids, where the morphology was found to be a function of the solvent and the adopted protocols. On similar lines, the polymeric adducts could provide interesting morphological information with different assembling protocols. Recently, sonochemistry has been used as a newer methodology for various useful applications, ranging from organic synthesis to polymerization and the degradation of surfactants or pollutants.¹¹ The ultrasonic treatment produces acoustic cavitations within the solution; these result in an increase in the pressure and temperature of the media,^{12,13} which may facilitate the formation of complex architectures during the self-assembly process by affecting both physical and chemical properties of the adducts (Figure 1).¹⁴

In this study, we showed that uniform nanorings of polymeric porphyrin and fullerene were preferentially and efficiently assembled with a sonication-induced self-assembly protocol. The hierarchical structure of these nanorings made it possible to characterize them even at the molecular level. The formation of uniform nanorings may provide further insights into the fabrication of advanced materials; additionally, this provides the possibility of further understanding the morphology of porphyrin–fullerene complexes under the influence of sonication with respect to the attached hydrophobic–hydrophilic polymers. Such hybrid nanocomposites might have enhanced mechanical and electrical properties with perfectly organized hierarchical structures and might be used in drug-delivery and smart materials.

EXPERIMENTAL

Materials and Characterization

Pyrrole, benzaldehyde, *p*-hydroxybenzaldehyde, and azobisisobutyronitrile (99%) were purchased from Sigma-Aldrich. *N,N*-Dicyclohexyl carbodiimide and 4-dimethyl aminopyridine were purchased from Aladdin Reagents and were used as received. Poly(ethylene oxide) (2000) was obtained from Aladdin, and Fullerene (C_{60} , 99.5%) was purchased from Bucky and was used as received. All of the solvents and other chemicals were purchased from Sinopharm Chemical Reagent Co., Ltd., and were used as received unless otherwise stated. The sonication of the

samples was performed on a Kudos SK1200H high-frequency ultrasonic cleaner. Absorption spectra were recorded on a Shimadzu UV-2550 ultraviolet–visible (UV–vis) spectrophotometer with a quartz cuvette, and emission spectra were recorded on a Varian's Cary Eclipse fluorescence spectrophotometer. Transmission electron microscopy (TEM) images were taken on a JEOL JEM 1400 electron microscope operated at 100 kV with carbon-coated copper grids. Atomic force microscopy images were recorded on a Hitachi S-4800 instrument (Japan) with freshly cleaved mica as the substrate.

Synthesis of the Adducts Monochelic Porphyrinic Polystyrene (MPPS) and Fullerene-End-Capped Polyethylene Oxide (F-PEO)

The synthesis and characterization of both of the adducts were already reported elsewhere.¹⁵ Briefly, MPPS was synthesized by a typical RAFT polymerization with azobisisobutyronitrile as an initiator, whereas F-PEO was synthesized via a $CuSO_4 \cdot 5H_2O$ assisted click reaction of C_{60} -alkyne and poly(ethylene oxide)- N_3 at room temperature.

Sonication-Induced Self-Assembly

The self-assembly of MPPS and F-PEO gave rise to unique fibrils and spheres in our previous investigation, where adducts were self-assembled in tetrahydrofuran (THF). In our further investigations of self-assembly protocols for the same adducts, interesting rings were observed as a result of the sonication-induced self-assembly of MPPS and F-PEO. Typically, dimethylformamide (DMF) stock solutions of MPPS and F-PEO were sonicated for 3–4 min before being mixed together and stirred for 2 h. The mixed solution of the adducts was then sonicated for 20 min at room temperature; this was followed by stirring for 4 h. Finally, the solution was dialyzed into THF and analyzed with TEM, UV–vis spectroscopy, and fluorescence spectroscopy. TEM demonstrated the formation of characteristic uniform nanorings of various sizes. As control experiments, the self-assembly of tetraphenyl porphyrin (TPP) with pristine C_{60} and F-PEO, respectively, was also performed to give further insight into the controlled formation of the nanorings.

RESULTS AND DISCUSSION

Mainly, porphyrin and fullerene have natural tendencies to form donor–acceptor complexes, which have many potential applications.¹⁶ The different morphologies corroborate the applications of such complexes. Nanorings of polymeric porphyrin and fullerene were self-assembled in DMF via sonication-assisted assembly protocols. In this study, we sought unique nanorings by subjecting the mixed solution of MPPS and F-PEO to sonication. Polymeric tails attached covalently with the porphyrin and fullerene molecules showed dramatic effects on the morphology of the assembled architecture and their applications. Previously,^{17,18} we found the decisive role of the number of polymeric arms in the morphology and optical properties of the self-assembled spheres and fibrils. The four-armed polymeric porphyrins, on complexing with pristine fullerene (C_{60}), gave uniform nanospheres, whereas the one-armed polymeric porphyrins gave spherical and fibril aggregates, depending on the nature of the fullerene and on the simple and

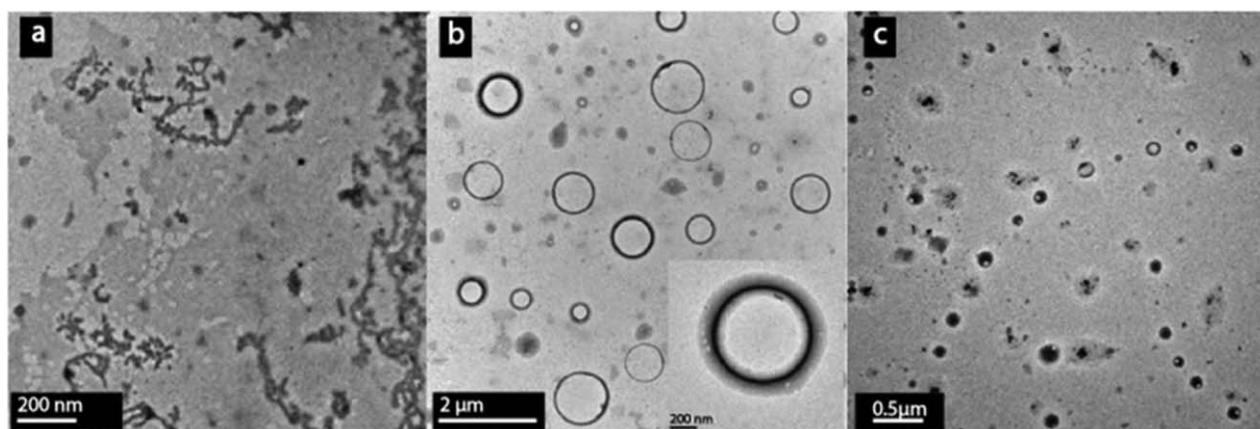


Figure 2. TEM images of the (a) self-assembled lateral aggregates, (b) nanorings, and (c) nanospheres of the MPPS and F-PEO complexes.

dropwise mixing of the porphyrinic and fullerenic solutions, respectively. In our further investigations of the self-assembly protocols for the same adducts, the sonication-induced self-assembly gave uniform rings. Evidence of the influence of sonication on nanoring formation was sought from the self-assembling of the adducts in the absence of sonication, where fibril formation occurred. Typically, the DMF stock solutions of MPPS and F-PEO were sonicated for 3–4 min before they were mixed together and stirred for 4 h. The mixed solution (with a 1:1 ratio of MPPS and F-PEO) of the adducts was then sonicated for 40 min at room temperature; this was followed by stirring for 4 h. Finally, the solution was dialyzed into THF and analyzed with TEM, UV–vis spectroscopy, and fluorescence spectroscopy. TEM demonstrated the formation of characteristic uniform nanorings of various sizes. As control experiments, the self-assembly of pristine TPP with F-PEO was also performed to obtain further insight into the controlled formation of nanorings. TEM revealed the presence of unique rings [Figure 2(b)]. The morphology of the assembled architectures were shown to

be dependent on the sonication time, as described in the schematic representation (Figure 1), and this played a vital role in the self-assembly process of ring formation, as in the absence of sonication, lateral aggregates were found [Figure 1(a)].

The rings were noticeably multimodal in nature, with sizes ranging from 100 to 1500 nm. The high-resolution TEM image [inset of Figure 2(b)] of these self-assembled rings gave further insight into the structure of these rings and indicated the soft peripheral surrounding a comparatively condense (darker) part about 35 nm in diameter. Apparently, the surroundings, lighter in color, consisted of an electronically less dense segment; this was the polymeric tail of the adduct, whereas the central darker part consisted of the electron-rich segments of the adducts. These were porphyrin and fullerene molecules. However, the rings were reshaped into spheres by the increasing sonication period [Figure 2(c)]. These observations suggest that the excess of sonication energy resulted in the ablation of rings into spheres followed by vesicle transformation. During sonication, the ultrasonic waves caused increases in the pressure, fluid

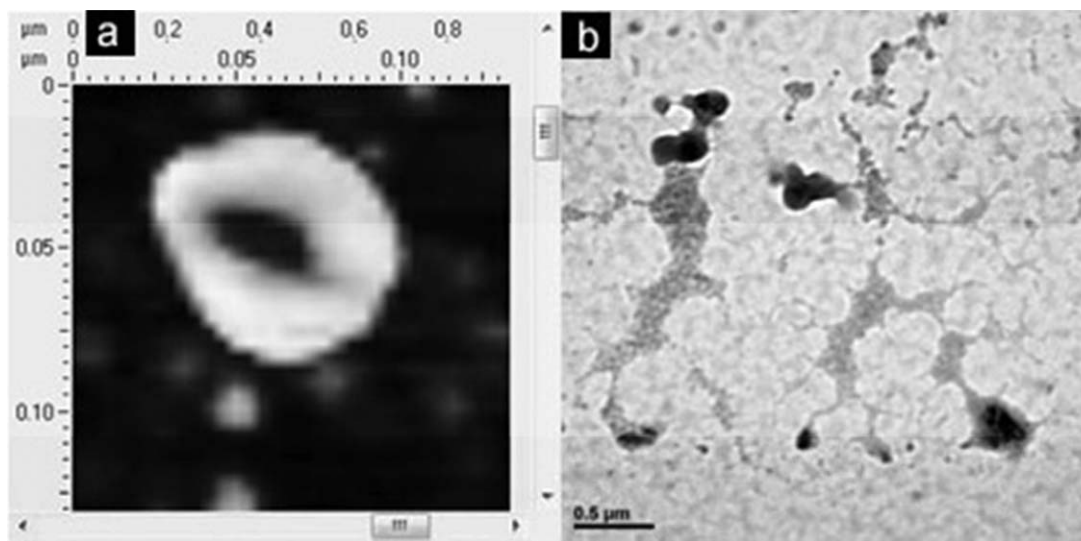


Figure 3. (a) Topographical image of a nanoring of the MPPS and F-PEO complexes under sonication and (b) TEM micrograph of irregular island-type aggregates of TPP and F-PEO.

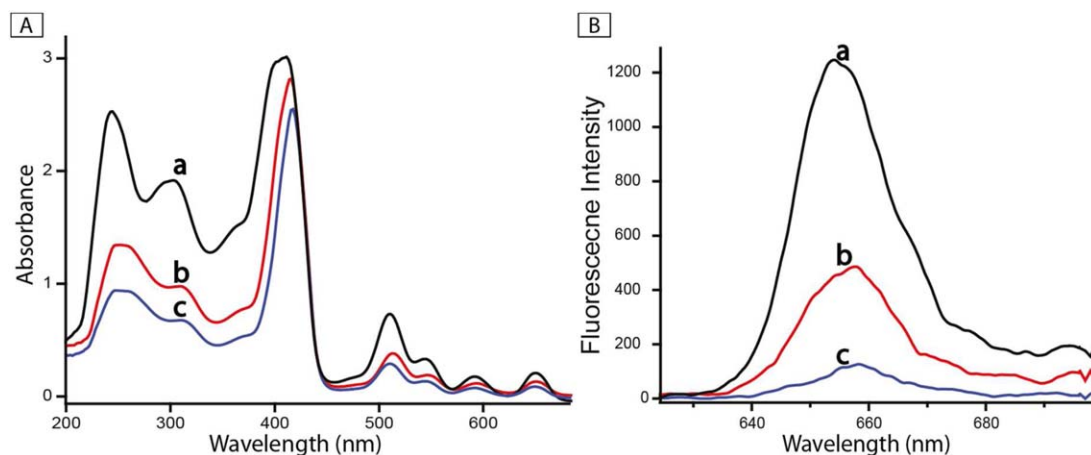


Figure 4. (A) UV-vis absorption and (B) fluorescence emission spectra of (a) MPPS, (b) MPPS-F-PEO rings, and (c) MPPS-F-PEO spheres in THF. [Color figure can be viewed in the online issue, which is available at wileyonlinelibrary.com.]

velocity, and temperature of the media¹²; this induced acoustic cavitation. The pressure amplitude of this ultrasonic excitation depended greatly on the sonication time and physical properties of the media¹⁹ and indicated that there was more stress in cases of longer sonication times. Hence, this transformation of the ring morphology to spheres might have been due to the higher localized stress of the medium caused by the larger acoustic cavitation associated with a greater sonication time. To further substantiate the nanoring formation, topographic scans of atomic force microscopy were performed in contact mode; this also confirmed the similar morphology [nanorings; Figure 3(a)].

Obvious nanorings with brighter peripheries and darker cores were observed in the atomic force microscopy topographic scan of the sample with mica as the substrate. The spectral studies of the assembling solutions also corroborated the molecular interactions of porphyrin-fullerene within the assembled architectures [Figure 4(A)]. The UV-vis spectra of the maiden MPPS showed one broad peak at 415 nm and four smaller peaks between 500 and 700 nm; these corresponded to the Soret and Q bands of the porphyrin. An obvious bathochromic shift (red-shift) in the Soret band of porphyrin on complexation with polymeric fullerene indicated the molecular interactions of porphyrin and fullerene. Similarly, a decrease in the absorbance intensity was also observed, and this also attested to the aforementioned interactions. The magnitude of the decrease in the absorption intensity for the rings and spheres were different; this might have been due to the three-dimensional packing in the spheres. This means that more electronic interactions were expected in the spherical morphology as compared to the rings (two-dimensional), and this caused a greater hypsochromic shift in the absorption spectra. Similarly, the fluorescence emission spectra of the maiden MPPS solution was quenched on complexation with polymeric fullerene, and the order of fluorescence quenching was identical with that of absorption magnitudes; this confirmed the complexation of porphyrin and fullerene,²⁰ as shown in Figure 4(B).

Furthermore, as control experiments on the complexation of F-PEO and TPP with the same protocol, irregular islandlike aggregates ending with lateral architectures were observed, as shown

in Figure 3(b). From these control experiments, it was clear that the polymeric arms significantly corroborated the unique morphology of the self-assembled architectures within similar self-assembling protocols. These studies show that the formation of uniform nanorings was critically associated with the polymeric nature of the adducts and the mode of their self-assembly.

CONCLUSIONS

In conclusion, this study provided important insights into the effect of the self-assembly protocol (the effects of sonication and polymeric arms) on the formation of nanofibrils and nanorings. We have described the hierarchical assembly methods of nanoring formation via the sonication-induced self-assembly of polymeric porphyrin and fullerene adducts. The morphology of the resulting architectures was studied with spectroscopic and microscopic methods in both the wet and dry phases. The key spectroscopic and microscopic data attested to the molecular interactions and morphology of these assembled architectures. These studies and protocols are expected to offer both new strategies for the synthesis and design of two-dimensional nanomaterials and an effective method to control the size and uniformity of the nanostructures through the optimization of several parameters. In this way, this protocol is expected to work for other raw materials and for the construction of unique architectures. Because of the facile fabrication process and uniform morphology, the resulting composite architectures may show promising applications in drug-delivery and advance materials.

ACKNOWLEDGMENTS

The authors acknowledge the startup financial support of the Higher Education Commission of Pakistan (contract grant number 21-329/SRGP).

REFERENCES

- Helmich, F.; Lee, C. C.; Nieuwenhuizen, M. M. L.; Gielen, J. C.; Christianen, P. C. M.; Larsen, A.; Fytas, G.; Leclère, P. E.

1. L. G.; Schenning, A. P. H. J.; Meijer, E. W. *Angew. Chem. Int. Ed.* **2010**, *49*, 3939.
2. Ling, S.; Li, C.; Adamcik, J.; Wang, S.; Shao, Z.; Chen, X.; Mezzenga, R. *ACS Macro Lett.* **2014**, *3*, 146.
3. Guldi, D. M.; Martin, N. *J. Mater. Chem.* **2002**, *12*, 1978.
4. Karaborni, S.; Esselink, K.; Hilbers, P. A. J.; Smit, B.; Karthaus, J.; van Os, N. M.; Zana, R. *Science* **1994**, *266*, 254.
5. Zhang, B.; Wang, D.; Li, M.; Li, Y.; Chen, X. *J. Appl. Polym. Sci.* **2012**, *126*, 2067.
6. Würthner, F.; Kaiser, T. E.; Saha-Möller, C. R. *Angew. Chem. Int. Ed.* **2011**, *50*, 3376.
7. Rong, Y.; Chen, P.; Liu, M. *Chem. Commun.* **2013**, *49*, 10498.
8. Balasubramanian, R.; Han, S.; Chamberlayne, C. *RSC Adv.* **2013**, *3*, 11525.
9. Natori, I.; Natori, S.; Hanawa, N.; Ogino, K. *J. Appl. Polym. Sci.* **2015**, *132*, 41629.
10. Wang, F.; Xu, L.; Nawaz, M. H.; Liu, F.; Zhang, W. *RSC Adv.* **2014**, *4*, 61378.
11. Skinner, E. K.; Whiffin, F. M.; Price, G. *J. Chem. Commun.* **2012**, *48*, 6800.
12. Ko, W.-B.; Heo, J.-Y.; Nam, J.-H.; Lee, K.-B. *Ultrasonics* **2004**, *41*, 727.
13. Pospisil, L.; Gal, M.; Hromadova, M.; Bulickova, J.; Kolivoska, V.; Cvacka, J.; Novakova, K.; Kavan, L.; Zupalova, M.; Dunsch, L. *Phys. Chem. Chem. Phys.* **2010**, *12*, 14095.
14. Zhang, J.; Han, B.; Liu, D.; Chen, J.; Liu, Z.; Mu, T.; Zhang, R.; Yang, G. *Phys. Chem. Chem. Phys.* **2004**, *6*, 2391.
15. Nawaz, M. H.; Xu, L.; Liu, F.; Zhang, W. *RSC Adv.* **2013**, *3*, 9206.
16. D'Souza, F.; Ito, O. *Chem. Commun.* **2009**, 4913.
17. Nawaz, M. H.; Xu, L.; Liu, F.; Zhang, W. *RSC Adv.* **2013**, *3*, 9206.
18. Nawaz, M. H.; Liu, J.; Liu, F.; Wang, X.; Zhang, W. *Mater. Lett.* **2013**, *91*, 71.
19. Coussios, C. C.; Farny, C. H.; Haar, G. T.; Roy, R. A. *Int. J. Hyperthermia* **2007**, *23*, 105.
20. Wang, R.; Gao, B.; Jiao, W.; Yu, L.; Pan, W. *J. Appl. Polym. Sci.* **2014**, *131*, 40516.